Resonant interference effects in the phonon Raman spectra of (311) GaAs/AlAs superlattices

A. J. Shields,* Z. V. Popović, M. Cardona, J. Spitzer, R. Nötzel, and K. Ploog†
Max-Planck-Institut für Festkörperforschung, Heisenbergstrasse 1, D-70569 Stuttgart, Federal Republic of Germany
(Received 17 August 1993)

We study the dependence on laser frequency (ω_L) of the Raman spectra of GaAs/AlAs superlattices (SL's) grown along the [311] direction. The observed phonon modes follow the polarization selection rules predicted by the SL crystal symmetry and, at the highest ω_L, the intensities predicted by the bulk Raman tensor. For lower ω_L we observe a complex variation in the intensities of the confined LO and TO modes which deviates sharply from these predictions. We interpret these deviations as due to interference between a background associated with the E_1 and $E_1 + \Delta_1$ gaps and a resonant contribution arising from the hh2 $\rightarrow$ $e2$ transition of the SL, both induced by the deformation potential interaction. For the latter, the electron-phonon coupling with the hole bands is diagonal, in contrast to the off-diagonal (hh$\rightarrow$lh) coupling of conventional (100) SL's. Evidence for a Fröhlich induced resonance at the $E_0 + \Delta_0$ gap of the SL's is also obtained.

I. INTRODUCTION

Phonon vibrations in semiconductors scatter electrons via the local change in the short range electronic potential that they create, a phenomenon known as the deformation potential interaction (DPI). In polar semiconductors there is an additional coupling for the longitudinal optic (LO) modes due to the electric fields set up by the separation of charge caused by the vibration, i.e., the Fröhlich interaction (FI). The FI with the electron and hole photoexcited in the Raman process almost cancel, because of their opposite charge, except for laser frequencies (ω_L) close to a transition between critical points in the band structure. The residual FI effect results from the different curvature of the bands involved.[1] Hence the FI is only significant for resonant photoexcitation. In GaAs, for photon energies above the $E_0 + \Delta_0$ gap, the dominant coupling was found to be due to the DPI associated with the E_1 and $E_1 + \Delta_1$ gaps.[1] Close to resonance with $E_0 + \Delta_0$, the DPI and FI were found to be roughly equal in strength, leading to interference between their contributions to the LO scattering amplitude.[2]

In GaAs/AlAs superlattices (SL's) the optic vibrations are restricted to individual layers by the difference in the cation masses. These confined optic phonons are labeled by an integer called the mode order describing their quantized k vector along the SL axis.[3] The symmetries of the DPI and FI Hamiltonian about the center of the well in GaAs/AlAs SL's (grown along the [100] direction) result in finite coupling for odd and even order LO modes, respectively.[4] This explains the observation of only even order modes for ω_L close to resonance with the band edge exciton where the FI dominates, while at ω_L's away from any resonances the DPI results in only odd modes.[4]

In this paper we study the ω_L dependence of the phonon Raman spectra of GaAs/AlAs SL's grown along the [311] direction. Consistent with previous measurements[4] we observe even order modes close to resonance with the hh1 $\rightarrow$ $e1$ of the SL, indicating the FI to be dominant for these ω_L. At the highest ω_L, away from any electronic resonance, we observe odd-order LO and TO modes with intensities in good agreement with the DPI Raman tensor for backscattering from the bulk (311) face. For intermediate ω_L's we observe an intriguing and complex variation of the intensities of the LO and TO confined modes. We explain this behavior as due to interference between the resonant contribution of the hh2 $\rightarrow$ $e2$ transition of the SL and a background associated with higher energy gaps. The fact that we observe the intensity of the *odd* order modes to resonate demonstrates that the coupling with the hh2 $\rightarrow$ $e2$ transition is due to DPI. We show that this resonant contribution to the DPI in (311) SL's involves intraband phonon scattering, in contrast to (100) SL's where only different valence bands can couple.

In a recent paper[5] we presented a study of the vibrational properties of GaAs/AlAs SL's grown along the [311] direction, comparing microscopic calculations to the phonon frequencies measured by Raman spectroscopy. In the Raman backscattering configuration a series of confined LO-like and TO-like modes can be observed. The LO modes, vibrating mainly along [311], are even with respect to the only symmetry element of these structures, namely, the (00$\bar{1}$) reflection plane (C_s point group), and thus mix with their TO counterparts of the same symmetry (A'), which nominally vibrate along [$\bar{2}$33]. The odd TO modes, vibrating along [01$\bar{1}$], are unmixed (A'' symmetry). The low symmetry of these structures al-

0163-1829/94/49(11)/7584(8)/$06.00

lows one to investigate in backscattering all three types of modes mentioned, in contrast to the more conventional [001]-grown systems where only LO modes can be observed. We present here the resonance behavior of these Raman modes in (311) SL's over a wide ω_L range. Resonant Raman data near the lowest direct gap (hh1 $\rightarrow$ e1) of (311) GaAs/AlAs SL's of somewhat larger period ($\gtrsim$ 30/30 monolayers) were reported earlier.[6] They yielded evidence for the lateral periodicity associated with these structures[7] in the form of a splitting of the various confined phonon peaks. The present work emphasizes the dependence of the scattered intensities above the hh1 $\rightarrow$ e1 gap and covers the laser energy range from 1.9 to 2.7 eV. No evidence for the lateral periodicity was obtained in the present work, probably due to the broader phonon linewidth observed in these narrower layers, as well as the weaker resonances, compared with the work in Ref. 6.

II. SYMMETRY, SELECTION RULES, AND ELECTRON-PHONON INTERACTION

Schematic projections of the Ga(Al)As layers onto the $(01\bar{1})$ and $(\bar{2}33)$ planes are shown in Figs. 1(a) and 1(b), respectively. Here we have adopted the convention for the $(311)A$ surface, that the cation atom occupies the origin of the bulk primitive unit cell, while the As atom is positioned at $a_0/4(111)$. [For the $(311)B$ surface the cation and anion must be interchanged.] A detailed knowledge of the surface under study is essential when considering interference effects between the various components of the Raman tensor, in particular deformation potential and Fröhlich contributions.[2,8] As already mentioned, a $(01\bar{1})$ mirror plane ($\sigma_{x'}$) is the only symmetry element, apart from the identity, of the C_s point group. Consequently, there are only two symmetry classifications of phonon modes, defining whether the vibration is preserved (labeled A') or inverted (A'') upon reflection on

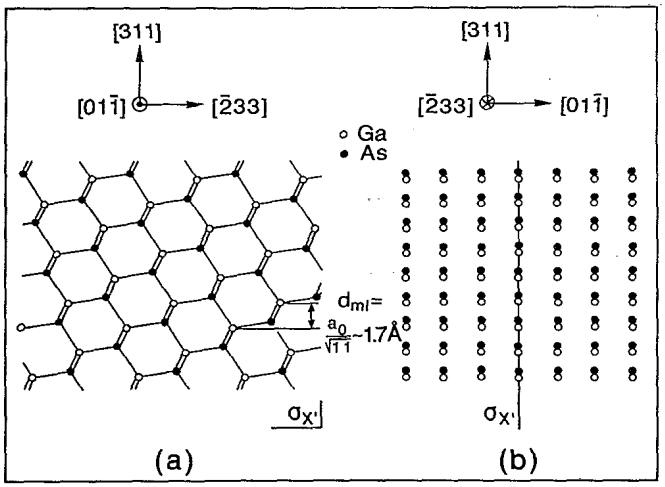

FIG. 1. Schematic diagram of the zinc-blende structure of bulk GaAs or AlAs projected onto the $(00\bar{1})$ and $(\bar{2}33)$ planes and the coordinate axes used in this work. Notice the mirror plane parallel to $(01\bar{1})$.

plane $\sigma_{x'}$. The pure transverse modes ($TO_{x'}$), vibrating perpendicular to the reflection plane, belong to A'', while the in-plane transverse ($TO_{y'}$) and longitudinal modes have A' symmetry and thus mix.

The Raman tensors describing the dipole-allowed scattering by the optical modes in the parent bulk crystals, expressed in the $(x' = [01\bar{1}], y' = [\bar{2}33], z' = [311])$ coordinate system, are

$$R_{x'} = \frac{1}{\sqrt{2}} \begin{pmatrix} 0 & -d & d \\ -d & 0 & 0 \\ d & 0 & 0 \end{pmatrix},$$
$$R_{y'} = \frac{1}{\sqrt{22}} \begin{pmatrix} 0 & 3d & 3d \\ 3d & 0 & -2d \\ 3d & -2d & 0 \end{pmatrix}, \quad (1)$$
$$R_{z'} = \frac{1}{\sqrt{11}} \begin{pmatrix} 0 & d & d \\ d & 0 & 3d \\ d & 3d & 0 \end{pmatrix}.$$

Dipole allowed scattering is usually related to deformation potential electron-phonon interaction (DPI), although for LO modes it also contains three-band Fröhlich interaction contributions.[1] For backscattering normal to the (311) face, the $R_{z'}$ tensor describes DPI plus some three-band Fröhlich contributions of the LO mode, while $R_{x'}$ and $R_{y'}$ represent DPI scattering by TO modes vibrating along the $[01\bar{1}]$ and $[\bar{2}33]$ directions, respectively. The dipole forbidden FI scattering by LO phonons is described by the tensor

$$R_{\mathrm{FI}} = \begin{pmatrix} a & 0 & 0 \\ 0 & a & 0 \\ 0 & 0 & a \end{pmatrix}. \quad (2)$$

The Raman-polarization selection rules for backscattering of the (311) surface resulting from these tensors are summarized in Table I, where $TO_{y'}$ and $LO_{z'}$ represent the case $k_z \rightarrow 0$. Notice that for the LO modes the DPI and two-band or intraband FI interfere additively and subtractively in $\bar{z}'(y', y')z'$ and $\bar{z}'(x', x')z'$ polarizations, respectively.[2,8] The same selection rules can be applied *off-resonance* to the (311) GaAs/AlAs SL's, in principle with no additional symmetry conditions on the order number (m) of the confined modes. Consequently, the A' modes are allowed regardless of whether m is odd or even for backscattering with the incident and scattered light polarized parallel to one another and either $[01\bar{1}]$ or $[\bar{2}33]$ axes. Similarly, A'' modes are, in principle, possible in depolarized geometry for both m odd and even.

The absence of a selection rule regarding the mode order (m) in (311) SL's contrasts with the situation in the most commonly studied (100) SL's, where twofold axes perpendicular to the growth direction exist. This symmetry element forces the confined phonon modes to be odd or even with respect to the twofold rotations, a fact which imposes further selection rules upon the electron-phonon interaction. For intraband scattering there is zero coupling to modes which have an antisymmetric interaction potential with respect to such rotations. Hence the FI and bulk DPI couple to only the m = even and m = odd modes, respectively. These selection rules have been ob-

TABLE I. Raman-polarization selection rules for backscattering normal to the (311) surface of GaAs. The values inside the square brackets represent the scattering amplitude with their signs. d is the Raman tensor component for DPI while a represents the Fröhlich interaction induced component.

Configuration	Polarization in	Polarization out	Raman cross section A'	Raman cross section A''
$\bar{z}'(x',x')z'$	$[01\bar{1}]$	$[01\bar{1}]$	$\left(+\sqrt{\frac{2}{11}}d\right)^2 \mathrm{TO}_{y'} + \left(-\frac{3}{\sqrt{11}}d + a\right)^2 \mathrm{LO}_{z'}$	0
$\bar{z}'(y',y')z'$	$[\bar{2}33]$	$[\bar{2}33]$	$\left(-\frac{54}{11\sqrt{22}}d\right)^2 \mathrm{TO}_{y'} + \left(+\frac{15}{11\sqrt{11}}d + a\right)^2 \mathrm{LO}_{z'}$	0
$\bar{z}'(x',y')z'$	$[01\bar{1}]$	$[\bar{2}33]$	0	$+\left(\sqrt{\frac{2}{11}}d\right)^2 \mathrm{TO}_{x'}$

served in the Raman spectra of (100) GaAs/AlAs SL's, which show only even modes under resonant photon excitation conditions and only odd modes when the photon energy is far from any electronic transition, explained by coupling due to the FI and DPI, respectively.[4] Note that this mode order selection rule for the coupling prevents interference between the DPI and FI contributions to the scattering amplitude, like that reported for bulk GaAs for resonance with $E_0 + \Delta_0$.[2]

This dependence of the electron-phonon coupling upon the mode order can be readily argued using perturbation theory. The matrix element describing the electron-phonon interaction is given by

$$M(m) = \int_{-\infty}^{+\infty} \psi_{a',n'}(z')\phi_m(z')\psi_{a,n}(z')\, dz' \,, \qquad (3)$$

where $\psi_{a,n}(z')$ is the electron envelope function of the nth subband associated with band a and $\phi_m(z')$ represents the electron-phonon interaction potential which contains components due to the FI and DPI. The bulk-like DPI is related to the local change in the short range electronic potential caused by the vibration and is consequently proportional to the atomic displacement of the mode $\phi_m^{\mathrm{DPI}}(z') \sim u_m(z')$. On the other hand, the FI is caused by the long range electric fields created by the separation of charge in LO vibrations of polar materials. Since the induced polarization (i.e., electric field) is proportional to the vibrational amplitude, its potential is determined by $\phi_m^{\mathrm{FI}}(z') \sim -\int u_m(z')dz'$.

In (100) SL's $u_m(z')$ is antisymmetric upon one of the twofold rotations for m = odd and symmetric for m = even. Since the Raman intensity is significant only for scattering between the same subband number (i.e., n=n') (otherwise one of the electron-photon matrix elements becomes negligible), the FI couples significantly only to the even order modes. In contrast, the symmetry of $\phi_m^{\mathrm{DPI}}(z')$ means that the DPI couples only to m=odd modes. In (311) SL's the lack of a corresponding twofold rotation axis strictly speaking removes this selection rule concerning the coupling of the odd and even order modes. We note, however, that even in the (311) SL case within the macroscopic approximation of Ref. 9, and under the assumption of isotropy to order q_m^2,[10] an approximate reflection plane exists perpendicular to the SL axis. The asymmetry of the vibrational modes of (311) SL's can be modeled by assuming, as usual, that the phonon envelope function does not vanish at the As boundary, but at the first cation plane of the barrier. From Fig. 1 one can deduce that the modes will penetrate farther into the "upper" barrier than "lower" one. Using such a model of the asymmetry we calculated its effect upon the DPI and FI matrix elements to be negligible, provided the layers are thicker than a few monolayers. Hence in (311) SL's it is still true that the DPI and FI favor the odd and even order modes, respectively.

There is, however, a more significant difference between the electron-phonon interaction in (100) and (311) SL's. In (100) SL's it can easily be shown that the diagonal coupling of the electronic states [i.e., *intra*band scattering, where a'=a in Eq. (3)] due to the DPI is zero. Hence Raman scattering in (100) SL's via the DPI involves the so-called three band terms,[1] with, for example, the phonon being scattered between the light and heavy hole bands. It is therefore relatively weak since both energy denominators do not vanish simultaneously, except, perhaps, in the so-called doubly resonant case, in which the splitting between hh-lh for a given n equals the phonon frequency.[11]

SL's without a twofold axis or a reflection plane perpendicular to the direction of growth (e.g., [111],[311]) have different symmetry behavior for the electron-phonon interaction. The LO phonons, for instance, are completely symmetric with respect to all operations of the point group, a fact which leads to diagonal electron-phonon matrix elements at the Brillouin zone center. The resonant scattering becomes of the two-band type, and this can lead to stronger resonances than those observed in the three-band, nondoubly resonant case. We shall show here that such effects, involving the hh2 $\rightarrow$ e2 transitions at the Γ point, play an important role in resonant Raman scattering in the (311) (17/17) SL under consideration.

The macroscopic selection rules of Table I are expected to apply to the (311) SL's only for ω_L away from any resonances. The effect of the lowered symmetry is in this case not important. It can be represented by small splittings of transition energies which will not be significant provided ω_L is away from those gaps. This is expected to be the case for the contribution to the scattering amplitude of the E_1 and $E_1 + \Delta_1$ gaps (at $\sim$3 eV for GaAs) in our ω_L region, which is known to be large for GaAs.[1] For ω_L in resonance with excitations between confined states related to the E_0 gap, however, one should see the effects of broken symmetry and the selection rules of Table I should not apply. As an example we mention that for

(100) SL's, and also for GaAs under stress, antisymmetric components of the Raman tensor, forbidden in bulk, can be observed.[11,12] We discuss below the DPI resonant contribution to the Raman tensor of a hh$n \rightarrow en$ transition which will be later used to interpret our data around the hh2 $\rightarrow e2$ gap.

We assume that the Luttinger parameters of the valence bands γ_2 and γ_3 are equal. This is a reasonable approximation for GaAs since $(\gamma_2-\gamma_3)/(\gamma_2+\gamma_3) \simeq 0.16$. This assumption leads to isotropy of the valence bands around Γ and thus to the result that the SL wave functions are angular-momentum-like even for the (311) case [for heavy hole (hh) and light hole (lh) bands, respectively]:

$$\begin{aligned}
&\left(+\frac{3}{2},+\frac{3}{2}\right) : \frac{1}{\sqrt{2}}(X'+iY')\uparrow , \\
&\left(+\frac{3}{2},-\frac{3}{2}\right) : \frac{1}{\sqrt{2}}(X'-iY')\downarrow ; \\
&\left(+\frac{3}{2},+\frac{1}{2}\right) : \frac{1}{\sqrt{6}}(X'+iY')\downarrow -\sqrt{\frac{2}{3}}Z'\uparrow , \\
&\left(+\frac{3}{2},-\frac{1}{2}\right) : \frac{1}{\sqrt{6}}(X'-iY')\uparrow +\sqrt{\frac{2}{3}}Z'\downarrow
\end{aligned} \tag{4}$$

where the $\uparrow$ ($\downarrow$) indicates spin up (down) and

$$\begin{aligned}
X' &= \frac{1}{\sqrt{2}}(Y-Z) , \\
Y' &= \frac{1}{\sqrt{22}}(-2X+3Y+3Z) , \\
Z' &= \frac{1}{\sqrt{11}}(3X+Y+Z) .
\end{aligned} \tag{5}$$

X, Y, Z represent the orbital wave functions of the bulk with the symmetries of the Cartesian axes.

The optical phonons of the bulk have x, y, z symmetry. It is easy to see from Eq. (4) with (X', Y', Z') replaced by (X, Y, Z) that such phonons do not couple the hh bands with themselves in the case of (100) SL's (i.e., no diagonal matrix elements of the electron-phonon interaction). This follows from the fact that the only nonzero matrix elements of the electron-phonon interaction have the form

$$D = \langle X | O_y | Z \rangle \tag{6}$$

plus circular permutations, where O_y represents the electron-phonon Hamiltonian for the phonon polarized along y.

If the orbital functions appropriate to the (311) SL are used [Eqs. (4) and (5)], however, it is straightforward to show that intraband terms appear for the $(3/2, \pm 3/2)$ and the $(3/2, \pm 1/2)$ bands. For the $(3/2, \pm 3/2)$ bands [quantization axis along (311)] the diagonal electron-phonon matrix elements are

$$\begin{aligned}
\left\langle \frac{3}{2},\frac{3}{2}\middle| O_{\mathrm{LO}} \middle|\frac{3}{2},\frac{3}{2}\right\rangle &= \frac{1}{2}\left[\langle X' | O_{\mathrm{LO}} | X' \rangle + \langle Y' | O_{\mathrm{LO}} | Y' \rangle\right] \\
&= -\frac{9D}{11\sqrt{11}} = -0.25D .
\end{aligned} \tag{7}$$

This expression can be either calculated directly, as indicated above, or simply obtained by considering that $\langle X' | O_{\mathrm{LO}} | X' \rangle$ and $\langle Y' | O_{\mathrm{LO}} | Y' \rangle$ are isomorphic to the scattering amplitudes of Table I for the (x', x') and (y', y') scattering configurations, respectively. Adding these amplitudes, taken from Table I, we recover indeed Eq. (7) provided we replace d by D. The same procedure can be used to obtain the scattering amplitudes for TO-like phonons. By adding the scattering amplitudes given in Table I for $\mathrm{TO}_{y'}$ phonons in (x', x') and (y', y') configuration we find

$$\left\langle \frac{3}{2},\frac{3}{2}\middle| O_{\mathrm{TO}_{y'}} \middle|\frac{3}{2},\frac{3}{2}\right\rangle = -\frac{16\,D}{11\sqrt{22}} = -0.31D . \tag{8}$$

The corresponding Raman tensor component is obtained by multiplying by the electron-photon matrix elements which connect these $(3/2, \pm 3/2)$ valence bands with the conduction bands. These matrix elements are the same for (x', x') and (y', y') scattering configurations. Hence the scattering amplitudes for the resonant contribution of hh$\rightarrow e$ transitions are proportional to Eqs. (7) and (8) for LO and $\mathrm{TO}_{y'}$ phonons, respectively, the same in both scattering configurations and very different indeed from the results of Table I. As shown above the diagonal electron-phonon matrix element for the intraband coupling to the hh bands can be simply obtained by averaging the scattering amplitudes of Table I for the (x', x') and (y', y') configurations and replacing d by D. This applies to either the LO or the $\mathrm{TO}_{y'}$ phonons. The $\mathrm{TO}_{x'}$ phonon does not couple the hh band to itself.

We notice that Eqs. (7) and (8) yield the electron-phonon matrix elements, and corresponding contributions to the Raman tensor, of the same sign for LO and TO scattering and also equal for (x', x'), and (y', y') polarizations. The nonresonant contributions of Table I reverse sign from LO to TO, and from (x', x') to (y', y') configuration. Hence constructive and destructive interferences must result. The observation of these interferences is the main result of this paper.

III. RAMAN SCATTERING SPECTRA

The (311) GaAs/AlAs SL's studied here have periods of (14/13), (17/17), and (25/28) monolayers, as determined by x-ray characterization.[5] We shall present in detail only the results for the (17/17) sample, since the interference effects to be discussed occur in the middle of our photon energy range for this structure. The results obtained for the other SL's are fully consistent with those for the (17/17) sample and with the interpretation presented here.

Figure 2 displays the GaAs-like optical modes measured for the (311) $(\mathrm{GaAs})_{17}/(\mathrm{AlAs})_{17}$ SL with the 4579 Å laser line and the three principal polarization configurations. Comparison with Table I reveals that the spectra follow the selection rules derived from the symmetry analysis, assuming bulklike Raman tensors and that the DPI dominates over the FI. This is expected for this photon energy which lies well above the E_0 gap

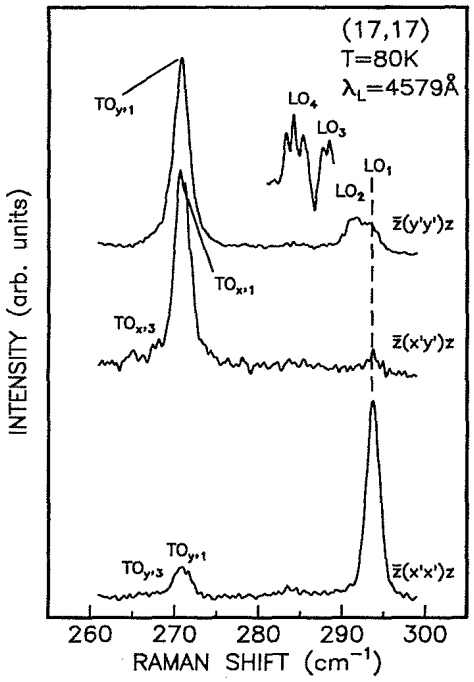

FIG. 2. Raman spectra of the GaAs optical phonon region measured on the (311) $(GaAs)_{17}/(AlAs)_{17}$ SL, at 80 K, with the 4579 Å laser line, away from all resonances, for different polarization geometries. The three spectra are scaled to have the same maximum height. The intensities of the LO and TO modes follow the selection rules outlined in Table I.

$[n = 1$ (~1.8 eV) and $n = 2$ (2.5 eV)] and below the E_1 gap (3 eV). In particular, for $\bar{z}'(y',y')z'$ polarizations the TO mode is much stronger than LO, while this ordering is reversed for $\bar{z}'(x',x')z'$. Crossed polarizations, $\bar{z}'(x',y')z'$, show a strong TO contribution, although there is also a rather insignificant LO feature, forbidden within the selection rules of the C_s group. Distinct features due to several mode orders are observable: $m = 1$–4 for LO and $m = 1,3$ for TO. The frequencies of these modes plotted against their effective k vector due to confinement map the bulk dispersions closely.[5]

Notice that in the LO region of the spectrum, the even order modes appear more clearly for $\bar{z}'(y',y')z'$ than for $\bar{z}'(x',x')z'$ polarizations. This is explained by the FI being stronger, relative to DPI, for the LO modes in $\bar{z}'(y',y')z'$ than in $\bar{z}'(x',x')z'$. As discussed in Sec. II, the approximate symmetry about the center plane of the well results in the even LO modes being favored by the FI and odd LO modes by the DPI of intrasubband scattering.

Figure 3 plots the two parallel polarization configurations measured for the AlAs-like optical phonons of the (311) $(GaAs)_{17}/(AlAs)_{17}$ SL with different lines of an Ar laser. Comparison with Table I reveals that the AlAs-like modes also follow the selection rules predicted for the DPI, with the TO modes being stronger than LO for $\bar{z}'(y',y')z'$ and LO dominating for $\bar{z}'(x',x')z'$ *throughout the whole frequency range.* There is also a broad feature between the bulk LO and TO frequencies attributable to the so-called "interface mode,"[3] the intensity of which increases with decreasing ω_L.

Raman spectra similar to those plotted in Figs. 2 and 3 were measured for the other (311) SL's studied [(14/13) and (25/28)], with several LO and TO peaks being observed in both the GaAs and AlAs regions, due to dif-

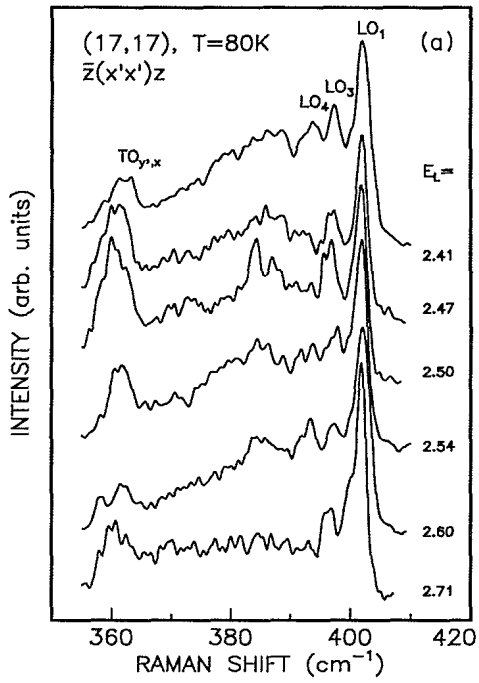

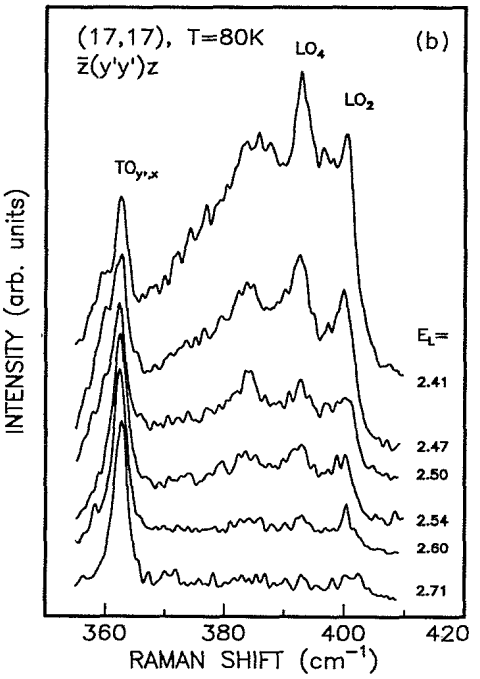

FIG. 3. Raman spectra of the AlAs region of the (311) $(GaAs)_{17}/(AlAs)_{17}$ SL, measured with the different lines of an Ar^+ laser for the $\bar{z}'(y',y')z'$ and $\bar{z}'(x',x')z'$ polarization geometries. The spectra are scaled to have the same maximum height. There is again good agreement with the predicted selection rules of Table I.

ferent confinement orders m. The results were rather similar to those represented in Figs. 2 and 3.

IV. RESONANT BEHAVIOR

We have observed a peculiar dependence of the GaAs-like optical Raman spectra upon the laser energy, centered in our ω_{LO} range for the $(GaAs)_{17}/(AlAs)_{17}$ SL but also present for the other samples. Figure 4 displays the Raman spectra measured with different lines of argon, krypton-ion, and dye lasers for $\bar{z}'(y',y')z'$ and $\bar{z}'(x',x')z'$ polarizations. At the highest laser energy (2.707 eV, 4579 Å) the spectra for the two polarizations follow the selection rules outlined in Table I: the TO and LO modes dominate for $\bar{z}'(y',y')z'$ and $\bar{z}'(x',x')z'$, respectively, as discussed in connection with Fig. 2. The LO_2 mode is stronger than LO_1 for $\bar{z}'(y',y')z'$ due to the FI dominating for this polarization, where the DPI is weaker (see Table I). At the lowest laser energy in Fig. 4 (1.915 eV, 6471 Å) the spectra in both polarizations are dominated by the even-order LO modes. The TO modes are weaker than the LO modes in both polarization geometries. This is explained by the intrasubband FI dominating ($a \gg d$) close to resonance with the $e1-hh1$ band edge transition and is consistent with previous measurements on (311) (Ref. 6) and (100) (Ref. 4) SL's. Both effective-mass Kronig-Penney calculations and microscopic linear combination of atomic orbitals[13] yield an $e1$-hh1 transition energy around 1.8 eV for this $(GaAs)_{17}/(AlAs)_{17}$ SL (see Table II).

It can be seen that there is a complex distortion of the Raman line shape at the intermediate laser energies in Fig. 4. In general, with decreasing laser energy from the highest value 2.707 eV, the LO modes strengthen relative to TO in $\bar{z}'(y',y')z'$, while the opposite trend is observed for $\bar{z}'(x',x')z'$. Figure 5 shows a plot of the intensities of LO_1 and LO_2 modes normalized to that of the TO mode for the two polarization configurations, as a function of laser energy. Notice that there is a maximum in the strength of LO_1 in $\bar{z}'(y',y')z'$ polarization near 2.5 eV and a corresponding minimum in $\bar{z}'(x',x')z'$. This is a clear indication of interference between different contributions to the Raman scattering amplitude of the LO mode, possibly of the type described in Sec. II. We ascribe the interfering amplitudes to a nonresonant background and a resonantly enhanced contribution for photon energies close to that of the hh2 $\rightarrow$ $e2$ transitions.

TABLE II. Calculated energies of several gaps at the Γ point of $(GaAs)_{17}/(AlAs)_{17}$ and $(GaAs)_{14}/(AlAs)_{13}$ SL's grown along [311].

	(17/17)		(14/13)	
$e1$-hh1	1.84[a]	1.78[b]	1.92[a]	1.83[b]
$e1$-lh1	1.89[a]	1.85[b]	1.98[a]	1.91[b]
$e2$-hh2	2.60[a]	2.69[b]	2.83[a]	2.79[b]
$e1$-so1	2.21[a]	2.16[b]	2.30[a]	2.23[b]

[a]Effective mass Kronig-Penney model.
[b]Tight binding model (Ref. 13).

We calculate (see Table II) the hh2 $\rightarrow$ $e2$ transition of the $(GaAs)_{17}/(AlAs)_{17}$ SL to lie at 2.60 eV.

Interference effects in the Raman intensities were also observed for the $(GaAs)_{14}/(AlAs)_{13}$ SL within our laser energy range but the resonant contribution is shifted to ~2.7 eV, which is at the limit of the frequency range

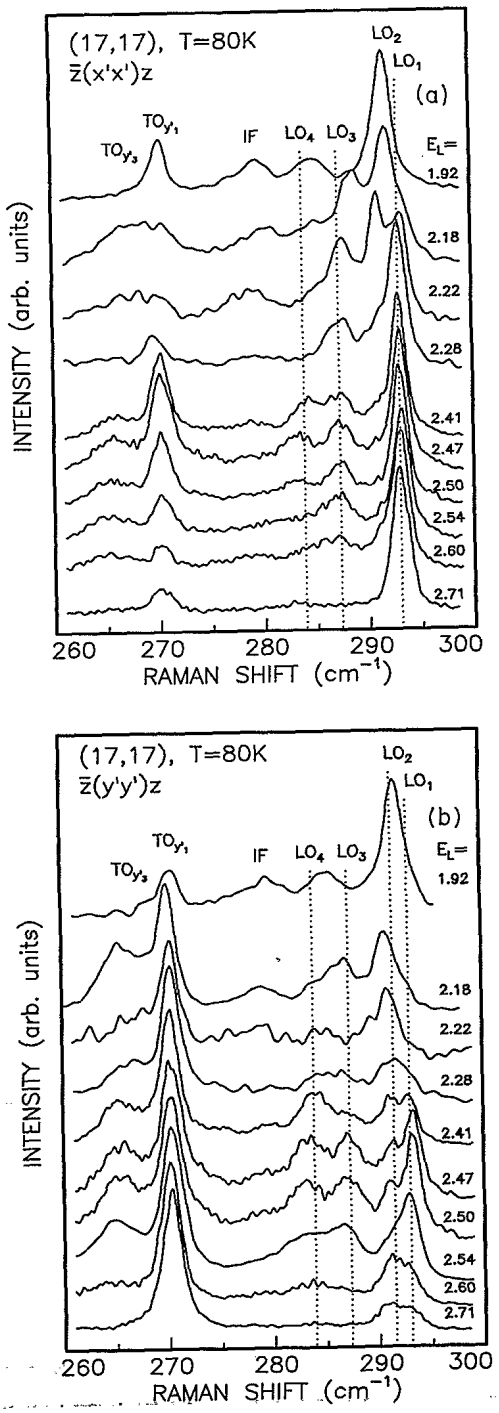

FIG. 4. The laser wavelength dependence of the GaAs-like optical phonon Raman spectra of the (311) $(GaAs)_{17}/(AlAs)_{17}$ SL for $\bar{z}'(y',y')z'$ and $\bar{z}'(x',x')z'$ polarization geometries. The spectra taken with the highest and lowest laser energy are dominated by the DPI and FI, respectively.

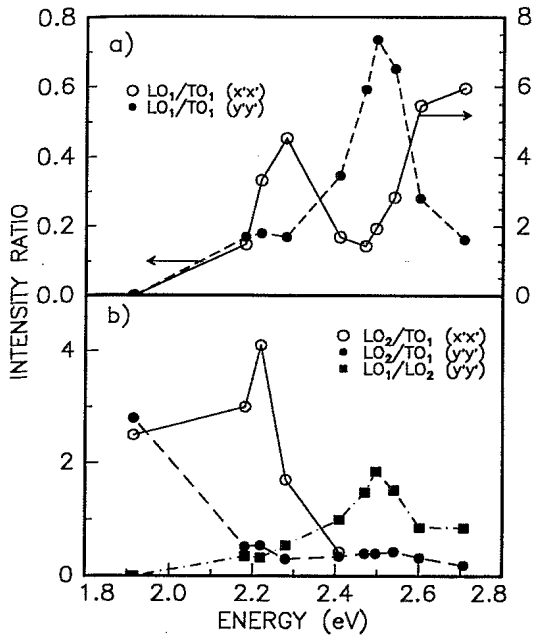

FIG. 5. The ratio of the intensity of (a) LO_1 to TO and (b) LO_2 to TO as a function of laser energy for the (311) $(GaAs)_{17}/(AlAs)_{17}$ SL.

we used. As for the previously discussed sample, this behavior is consistent with interference between a background and a hh2 $\rightarrow$ $e2$ resonant contribution which the calculation yields to lie at the energy of $\sim$2.8 eV for the $(GaAs)_{14}/(AlAs)_{13}$ SL (see Table II).

Interesting resonance effects appear also for the FI-induced LO_2 modes when normalized to their deformation potential counterpart [Fig. 5(b)]. Note that the LO_2/TO ratios exhibit a peak at $\sim$2.2 eV. Subject to further confirmation, we attribute this peak to transitions between the spin-orbit split $(1/2, \pm 1/2)$ valence bands and the $e1$ conduction band (see Table II). Another interesting feature of Fig. 5(b) is the peak in the LO_1/LO_2 ratio at 2.5 eV, i.e., at the hh2 $\rightarrow$ $e2$ transition energy.

V. DISCUSSION

The ingredients required for the understanding of the interesting resonance interference phenomena displayed in Figs. 4 and 5 have been presented in Sec. II. We first note that such effects are absent in the AlAs-like confined modes (Fig. 3) in agreement with their assignment to constructive and destructive interferences between a background and a resonant interband transition of the *GaAs layer*. The AlAs-like modes are not expected to couple to the latter and hence no interference should appear. However, we do observe some change in the AlAs-like interface mode with ω_L, explained by the penetration of its interaction potential into the GaAs layers.

The striking nature of the phenomenon displayed in Fig. 5 compels us to predict the sign (constructive vs destructive) expected for the interferences, i.e., the relative sign of the background and resonant contributions. The background is known to be due mainly to the E_1, $E_1+\Delta_1$ transitions which have their critical point at $\sim$3 eV in the bulk.[1] This critical point is not expected to be significantly modified in the SL's.[14] In the ω_{LO} region of our work, below the E_1 gap, the DPI E_1, $E_1+\Delta_1$ contribution to the Raman tensor d is supposed to be real.[15] For the standard definition of the corresponding deformation potentials and phonon displacements, this real contribution to d can be shown to be positive (this means that the $\varepsilon_r(\omega)$ increases along [111] for a positive sublattice displacement along [111]). The sign of the displacement of the hh states upon a positive sublattice displacement corresponding to the LO and $TO_{y'}$ phonons of the (311) SL under consideration can be inferred from Eqs. (7) and (8), where D is to be taken as positive.[1] We assume that the contributions to the susceptibility of hh2 $\rightarrow$ $e2$ transitions are excitonlike and thus can be represented by a Lorentzian function $L(\omega)$. Only its real part $L_r(\omega)$ will interfere with *real* and *positive* background of the E_1, $E_1+\Delta_1$ transitions. We approximate the resonant contribution to the scattering amplitude in the standard way by

$$W = -\frac{dL}{d\omega}\frac{d\omega_{0,2}}{du}\,, \tag{9}$$

where $\omega_{0,2}$ represents the hh2 $\rightarrow$ $e2$ gap and u the positive sublattice displacement. The diagonal electron-phonon matrix element $d\omega_{0,2}/du$ can be obtained from Eqs. (7) and (8) by reversing its sign (so as to take into account that $\omega_{0,2}$ is the conduction state energy *minus* that of the valence state): the constant D is proportional to the well-known electron phonon coupling constant d_0 (see Ref. 1) and is thus to be taken as positive. Hence the contribution W of Eq. (9) should have a sign opposite to that of $dL/d\omega$, for either LO or $TO_{y'}$, (x', x'), or (y', y') polarizations. The scattering amplitudes resulting from the interference between the two mechanisms, with the signs determined above, are shown schematically in Fig. 6. They represent remarkably well the phenomena shown in Figs. 4 and 5.

While the main features of these phenomena are accounted for by this theory, some other details are worth mentioning. First of all the possible resonance in the LO_2/TO_1 ratio observed near the spin-orbit split gap so1 $\rightarrow$ $e1$ ($\sim$2.2 eV, see Table II). In the bulk the DPI resonance at this gap is barely noticeable,[2] a fact which should also apply to GaAs since diagonal electron-phonon matrix elements vanish at the so1 band [this can be shown for the split-off band, i.e., $(1/2, \pm 1/2)$ band in the way followed in Sec. II]. The FI, however, has strong diagonal matrix elements at any state for LO_m with even m (e.g., LO_2). Hence the peak in the ratio LO_2/TO_1 at the so1 $\rightarrow$ $e1$ gap.

Another striking fact is the large strength of the LO_3 and TO_3 modes relative to their $m = 1$ counterparts close to resonance with the hh2 $\rightarrow$ $e2$ transition. This is simply because the m=3 mode couples more strongly to the n=2 envelope function than n=1. A similar phenomenon has been observed for the Raman intensity of acoustic phonons: in resonance with the hh2 $\rightarrow$ $e2$

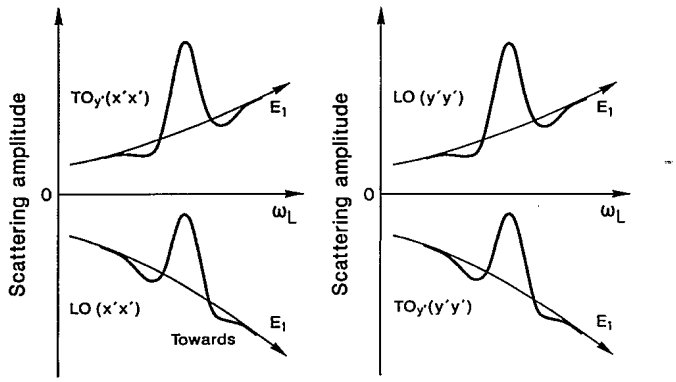

FIG. 6. Schematic diagram of the *amplitudes* for Raman scattering by LO and $TO_{y'}$ phonons in a GaAs/AlAs SL grown along [311]. The scattering efficiencies obtained by squaring these amplitudes represent rather well the results of Figs. 4 and 5.

gap the folded LA_3 modes are even stronger than their LA_1 counterparts.[16] Assuming perfect confinement to the GaAs layers of both the phonon and electron envelope functions, the electron-phonon matrix element of Eq. (3) due to the DPI is given by[16]

$$M(m,n,n'=n)=\frac{4n^2}{4n^2-m^2}\frac{\sin\frac{\pi m}{2}}{\frac{\pi m}{2}}\,\delta\,, \qquad (10)$$

where δ is a deformation potential constant. The scattered intensities are proportional to the square of Eq. (10), i.e., to

	$n=1$	$n=2$
$m=1$	0.72	0.46
$m=3$	0.03	0.23

(11)

Equation (11) indicates that while the $m=3$ mode is 20 times weaker than $m=1$ at the $n=1$ resonance, it has as much as half the strength of $m=1$ for the $n=2$ resonance. In the nonresonant case the ratio of intensities is expected to be $1^2/3^2 \simeq 0.11$. The ratio of strengths of the $m=1$ and $m=3$ modes (both LO and TO), shown in Fig. 4 in the resonant region, is in excellent agreement with these considerations.

VI. CONCLUSIONS

We have studied Raman resonance effects for GaAs-like phonons in (311) GaAs/AlAs SL's in the 1.9 – 2.7 eV region which include the $E_0+\Delta_0$ gap and the hh2 $\rightarrow$ $e2$ transitions. Strong deviations from the selection rules derived from the bulk Raman tensor are observed around the hh2 $\rightarrow$ $e2$ transitions. They result from interferences between a background scattering amplitude (stemming from the E_1, $E_1+\Delta_1$ transitions) and the resonant contribution of the hh2 $\rightarrow$ $e2$ gap confined to the GaAs layers. The relative sign of the interfering contributions has been calculated and found to agree with the experimental results for both LO and $TO_{y'}$ phonons in the (x',x') and (y',y') scattering configurations.

ACKNOWLEDGMENTS

Thanks are due to V. R. Velasco and F. García-Moliner for providing us with the tight binding data of Table II. We are indebted to P. Wurster, M. Siemers, and H. Hirt for technical assistance. A.J.S. and Z.V.P. thank the Royal Society (United Kingdom) and European Community, respectively, for financial support.

* Present address: Toshiba Cambridge Research Center, 20 Science Park, Milton Road, Cambridge CB4 4WE, United Kingdom.
† Present address: Paul-Drude-Institut für Festkörperelektronik, Hausvogteiplatz 5-7, D-10117 Berlin, Germany.

[1] M. Cardona, in *Light Scattering in Solids II*, edited by M. Cardona and G. Güntherodt, Topics in Applied Physics Vol. 50 (Springer, Heidelberg, 1982), p. 19.
[2] J. Menéndez and M. Cardona, Phys. Rev. Lett. **51**, 1297 (1983).
[3] For a review see B. Jusserand and M. Cardona, in *Light Scattering in Solids V*, edited by M. Cardona and G. Güntherodt, Topics in Applied Physics Vol. 66 (Springer, Heidelberg, 1989), p. 49.
[4] A.K. Sood, J. Menéndez, M. Cardona, and K. Ploog, Phys. Rev. Lett. **54**, 2111 (1985).
[5] Z.V. Popović, E. Richter, J. Spitzer, M. Cardona, A.J. Shields, R. Nötzel, and K. Ploog, preceding paper, Phys. Rev. B **49**, 7577 (1994).
[6] A.J. Shields, R. Nötzel, M. Cardona, L. Däweritz, and K. Ploog, Appl. Phys. Lett. **60**, 2537 (1992).
[7] R. Nötzel, L. Däweritz, and K. Ploog, Phys. Rev. B **46**, 4736 (1992).
[8] A. Cantarero, C. Trallero-Giner, and M. Cardona, Phys. Rev. B **40**, 12 290 (1989).
[9] C. Trallero-Giner, F. García-Moliner, V.R. Velasco, and M. Cardona, Phys. Rev. B **45**, 11 944 (1992).
[10] M. Chamberlain, M. Cardona, and B.K. Ridley, Phys. Rev. B **48**, 14 356 (1993).
[11] R.C. Miller, D.A. Kleinman, C.W. Tu, and S.K. Sputz, Phys. Rev. B **34**, 7444 (1986).
[12] F. Cerdeira, E. Anastassakis, W. Kauschke, and M. Cardona, Phys. Rev. Lett. **57**, 3209 (1986).
[13] D.A. Contreras-Solorio, V.R. Velasco, and F. García-Moliner, Phys. Rev. B **47**, 4651 (1993); V.R. Valesco (private communication).
[14] M. Garriga, M. Cardona, N.E. Christensen, P. Lautenschlager, T. Isu, and K. Ploog, Phys. Rev. B **36**, 3254 (1987).
[15] See Eq. 2.201 of Ref. 1. Note that the sign in the right-hand side of this equation should be + instead of −.
[16] V.F. Sapega, V.I. Belitsky, A.J. Shields, T. Ruf, M. Cardona, and K. Ploog, Solid State Commun. **11**, 1039 (1992).